Measuring the size of tubules in phloem and xylem of plants

Amelia Carolina Sparavigna

PHILICA. Article number 1104. Published on 29th August, 2017

Measuring the size of tubules in phloem and xylem of plants

Amelia Carolina Sparavigna
Department of Applied Science and Technology, Politecnico di Torino, Italy

The paper is showing how to measure, by means of the segmentation of a SEM image, the cross-sections of the tubules in phloem and xylem of plants.

Keywords: Image processing, Segmentation of images, Size of domains, Vascular plants.

The scanning electron microscope is necessary for revealing the fascinating world of the plants in their smallest structures. The complex vascular system of them appears in SEM micrographs as in the Figure 1, for instance. The figure is showing an image obtained by Louisa Howard, at the Dartmouth College EM facility. The image is available at the site www.cellimagelibrary.org [1]. It is showing a Nicotiana alata stem cross-section. In the Figure 1, we can see the outer epidermal layer; then we have the cortex and the large vascular bundles. As explained in the description of the image, the vascular bundles contain the phloem, which is nearest the cortex, and the xylem. Besides being very beautiful, the image is very interesting and seems useful for an elaboration, by means of an image processing, to evaluate the size of the cross-sections of the vessels that we find in it.

Before the processing of the image, with a short discussion of the related method based on the image segmentation, let us write a few words on the vascular plants. These plants have in their vascular system two different types of transport tissues. The xylem moves water and solutes from the roots to the leaves, whereas the phloem moves the soluble organic compounds created by photosynthesis, such as the sucrose [2], from the leaves to the rest of the plant. As explained in [3], xylem is a highly specialized tissue, which is providing, besides the transport of the water, the mechanical support to the plant. It is also transporting the hormonal signals in the plant. Actually, xylem is the most abundant biological tissue on earth [3].

Reference 4 illustrates the difference between phloem and xylem vascular systems. In phloem, the structure is elongated, having a tubular organization with thin walled sieve tubes. "The sieve tubes have pores at each end in the cross walls and microtubules that extend between sieve elements allowing longitudinal flow of material" [4]. The xylem has a structure having a tubular shape with no cross walls; in this manner it is allowing a continuous column of water inside, facilitating a more rapid transport within the xylem vessels.

The study of phloem and xylem is not easy for a researcher who has not a specific knowledge about plants. At the same time, it is also difficult to find and survey, among the many publications on the subject, all the methods of image processing applied to the study of the vascular system of plants or to the study of the plants in general. Therefore, I mention only a few references [5-9]: some of them are using the image segmentation.

For the reasons previously told, let us just address a simple problem: that of measuring the size of the tubules in phloem and xylem of the plant that we can see in the Figure 1.

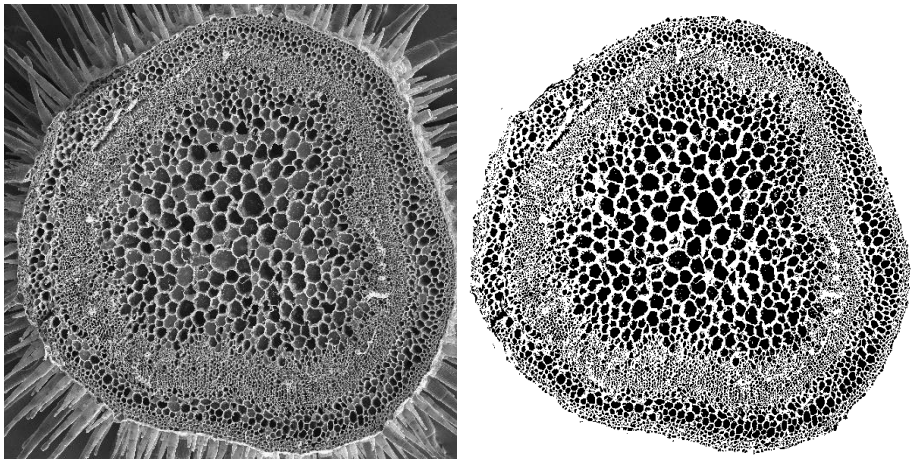

Figure 1: SEM image obtained by Louisa Howard (Dartmouth College EM facility), image available at http://www.cellimagelibrary.org/images/39340 (on the left), and a possible binary (black and white) image of it (on the right). In the binary image, the structures around the stem have been removed.

In image processing, a segmentation is a process of partitioning an image into multiple sets of pixels, that is, into some domains defined as “super-pixels”, in order to have a representation which is simpler than the original one and more useful to the following desired analyses [10-14]. The typical use of the image segmentation is that of locate objects (the domains), and find the boundaries among them. Specifically, the segmentation is a process of assigning a label to every pixel in an image, such that the pixels having the same label share certain characteristics [14]. Consequently, the result of the segmentation is a set of "segments" or “super-pixels”, covering the whole image.

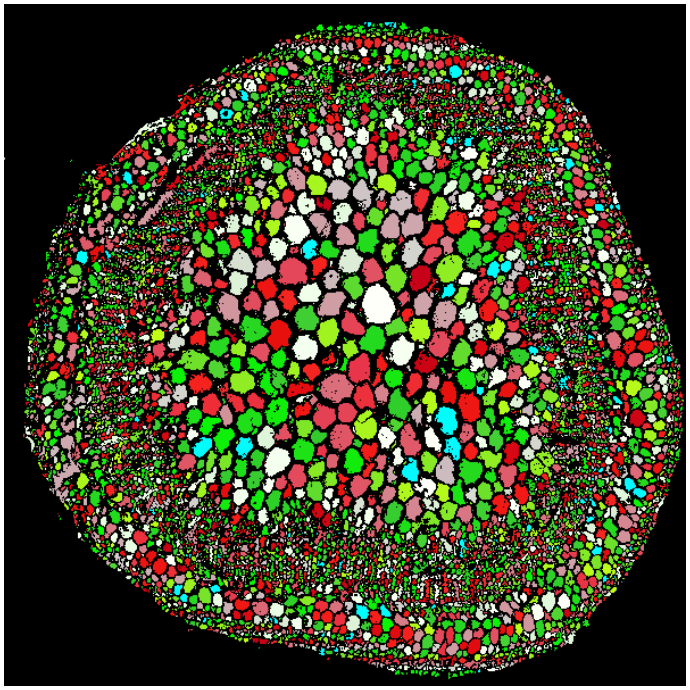

Figure 2: Result of the segmentation of the binary image in the Figure 1. Each domain (super-pixel) has a different colour. Each super-pixel corresponds to a cross-section of a tubule in the stem.

The segmentation that we use here is based on the binarization of the image. That is, the grey-tone image is modified into a black and white image. Then, the black domains are identified as the super-pixels (for the details of the segmentation, please see [15-18]). One of the possible binary images that we can use is shown in the Figure 1. The result of the segmentation is given in the Figure 2. Each domain (super-pixel) has a different colour. Each domain corresponds to a cross-section of a tubule in the stem.
After having determined the coloured domains, it is easy to obtain the size of each of them. The size is the number of pixels contained in the domain. If we have the possibility to know the measure, in microns, of the image size, it is very simple to estimate the area (in microns) of the domains. Moreover, we can determine the distribution of the domains, that is, the distribution of the cross-sections of the tubules in the SEM image, by counting them according to their area within intervals spaced of a certain amount of pixels. Here the original image is scaled to 600x600 pixels, in order to reduce the time of computation, and the areas are spaced of 10 pixels. We obtain the distribution given in the Figure 3.

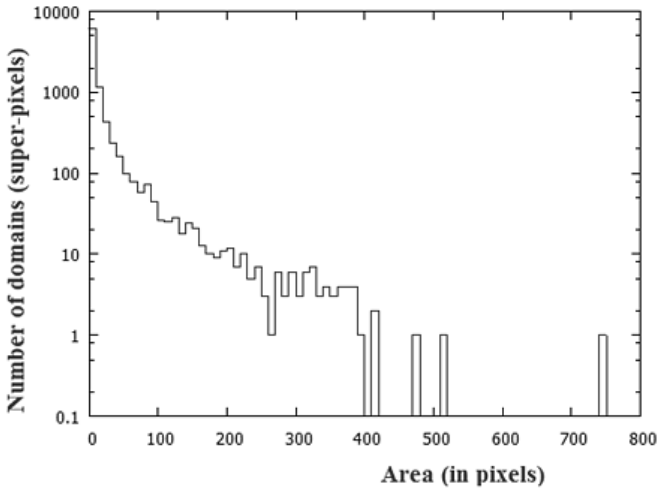

Figure 3: Distribution of the size of domains. We have only one domain having an area comprised between 740 and 750 pixels. It is the central white domain in the Figure 2.

As we can see, there is a large amount of very small domains. We can try to remove them. Actually, in the Figure 1, we see one of the possible binary images that we can have from the grey-tone image. The binary image was obtained using GIMP software, by means of a simple thresholding (the GIMP Threshold tool transforms an image into a black and white image, where white pixels represent the pixels of the image whose value is above the threshold, and black pixels represent pixels with value is below the threshold). In the Figure 1, the threshold was determined to have the best choice, according to a direct visual observation. However, we can apply to the binary image in Fig.1 a further filtering action, in order to have another binary image. First, we can use the ERODE filter, which widens and enhances bright areas of the image. Then a further filter is applied: it is the DILATE filter, which widens and enhances dark areas of the image. The binary image, which is resulting, is given in the Figure 4. We have strongly reduced the presence of the smallest domains. The Figure 4 is also showing the coloured segmentation of it.

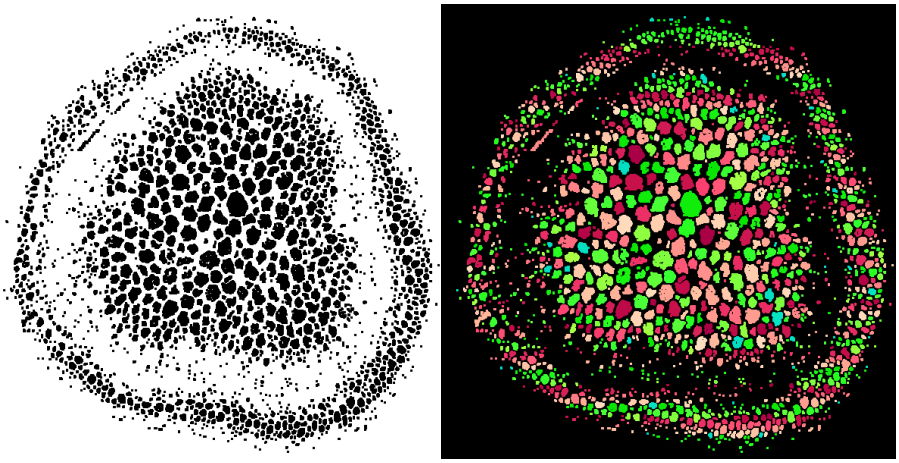

Figure 4: Another segmentation of the image in the Figure 1, using a different black and white image.

Therefore, to have the binary image in Fig.4, we have considered the binary image I from Fig.1. We filter it using ERODE obtaining an image I', then I' is filtered using DILATE, obtaining the image I'' shown in the Figure 4. Actually: I → ERODE → I' → DILATE → I''. Then I'' is segmented as in the Figure 4 on the right.

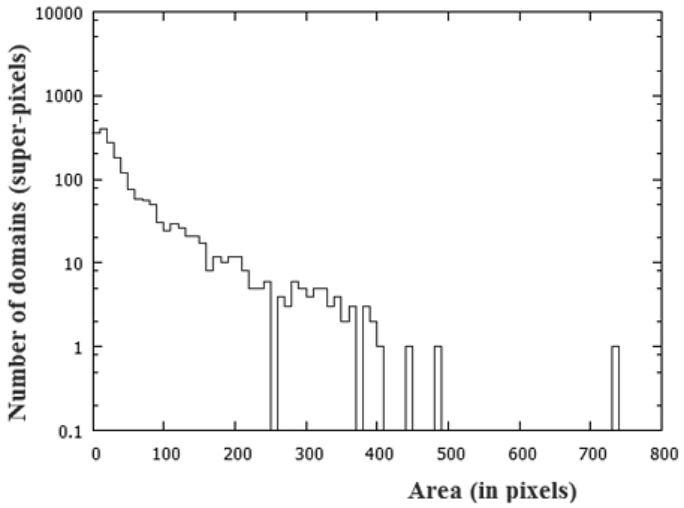

Figure 5: Distribution of the size of domains for the segmentation in the Figure 4.

We can also give the distribution of the size of domains (Figure 5). As we can see from this Figure, the size and number of the large domains is slightly affected by the further filtering (only two domains are modified of about 20 pixels), whereas the smallest domains are removed. We can see the comparison in the Figure 6.

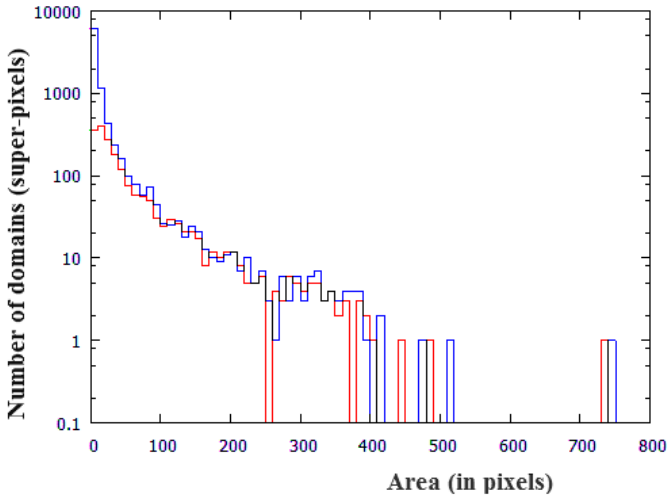

Figure 6: Comparison of the distributions. The distribution in the Figure 3 is here given in blue, whereas that of the Figure 5 in red.

Naively, I could tell that the domains removed by the second binarization are those corresponding to phloem, and that, in this manner, I could evaluate the number of phloem tubules in the stem by means of a difference of the distributions in Fig.6. Of course, a researcher who is studying the vascular system of the plants can infer proper conclusions from the distributions given in the previous figures (let us consider that detailed analyses of specific areas of the Figure 1 are possible too). Here we just tell that the method proposed in [15-18] could be of some interest also for researches concerning the plants.

References

[1] Louisa Howard. Nicotiana alata, Plant stem organization. Image available from www.cellimagelibrary.org at http://www.cellimagelibrary.org/images/39340

[2] Lalonde, S. Wipf, D., & Frommer, W.B. (2004). Transport mechanisms for organic forms of carbon and nitrogen between source and sink. Annu. Rev. Plant Biol. 55, 341–72. PMID 15377224. DOI: 10.1146/annurev.arplant.55.031903.141758

[3] Myburg, A. A., Lev-Yadun, S., & Sederoff, R. R. (2013). Xylem structure and function. ENCYCLOPEDIA OF LIFE SCIENCES. DOI: 10.1002/9780470015902.a0001302.pub2

[4] “Phloem vs. Xylem”. Diffen.com. http://www.diffen.com/difference/Phloem_vs_Xylem

[5] Bussières, P. (2014). Estimating the number and size of phloem sieve plate pores using longitudinal views and geometric reconstruction, Scientific Reports 4, Article number: 4929 (2014), DOI: 10.1038/srep04929

[6] Midorikawa, Y., & Fujita, M. (2005). Transverse shape analysis of xylem ground tissues by the Fourier transform image analysis, 3: Shape reconstruction of earlywood tracheids in 22 species and some parameters for normalizing cell shapes. Mokuzai Gakkaishi, Journal of the Japan Wood Research Society (Japan), 51(4), 218-226. DOI: 10.2488/jwrs.51.218

[7] Mallik, A., Tarrío-Saavedra, J., Francisco-Fernández, M., & Naya, S. (2011). Classification of wood micrographs by image segmentation. Chemometrics and intelligent laboratory systems, 107(2), 351-362. DOI: 10.1016/j.chemolab.2011.05.005

[8] Shen Pan, & Kudo, M. (2011). Segmentation of pores in wood microscopic images based on mathematical morphology with a variable structuring element. Computers and Electronics in Agriculture, 75(2), 250-260. DOI: DOI: 10.1016/j.compag.2010.11.010
[9] Dhondt, S., Van Haerenborgh, D., Van Cauwenbergh, C., Merks, R. M., Philips, W., Beemster, G. T., & Inzé, D. (2012). Quantitative analysis of venation patterns of Arabidopsis leaves by supervised image analysis. The Plant Journal, 69(3), 553-563. DOI: 10.1111/j.1365-313X.2011.04803.x
[10] Vv. Aa., Wikipedia, https://en.wikipedia.org/wiki/Microcellular_plastic. Retrieved 2017-02-04.
[11] Shapiro, L. G., & Stockman, G. C. (2001). Computer vision, New Jersey, Prentice-Hall, ISBN 0-13-030796-3
[12] Pham, D. L., Xu, Chenyang, & Prince, J. L. (2000). Current methods in medical image segmentation. Annual Review of Biomedical Engineering 2, 315–337. DOI: 10.1146/annurev.bioeng.2.1.315. PMID 11701515.
[13] Forghani, M., Forouzanfar, M., & Teshnehlab, M. (2010). Parameter optimization of improved fuzzy c-means clustering algorithm for brain MR image segmentation. Engineering Applications of Artificial Intelligence, 23 (2): 160–168. DOI: 10.1016/j.engappai.2009.10.002
[14] Vv. Aa. (2016). Wikipedia. https://en.wikipedia.org/wiki/Image_segmentation
[15] Sparavigna, A. C. (2017). Image Segmentation Applied to the Study of Micrographs of Cellular Solids, International Journal of Sciences, 6(2), 68-76. DOI: 10.18483/ijSci.1201
[16] Sparavigna, A. C. (2017). Image segmentation applied to micrographs of microcellular plastics. Philica, 2017, n.953. <hal-01456692>
[17] Sparavigna, A. C. (2016). Analysis of a natural honeycomb by means of an image segmentation. Philica, 2016, n.897. <hal-01416832>
[18] Sparavigna, A. C. (2016). A method for the segmentation of images based on thresholding and applied to vesicular textures. arXiv preprint arXiv:1612.01131.